NEURODEVELOPMENT

Hypothalamic regulation of regionally distinct adult neural stem cells and neurogenesis

Alex Paul,[1,2] Zayna Chaker,[3] Fiona Doetsch[2,3]*

Neural stem cells (NSCs) in specialized niches in the adult mammalian brain generate neurons throughout life. NSCs in the adult mouse ventricular-subventricular zone (V-SVZ) exhibit a regional identity and, depending on their location, generate distinct olfactory bulb interneuron subtypes. Here, we show that the hypothalamus, a brain area regulating physiological states, provides long-range regionalized input to the V-SVZ niche and can regulate specific NSC subpopulations. Hypothalamic proopiomelanocortin neurons selectively innervate the anterior ventral V-SVZ and promote the proliferation of Nkx2.1$^+$ NSCs and the generation of deep granule neurons. Accordingly, hunger and satiety regulate adult neurogenesis by modulating the activity of this hypothalamic–V-SVZ connection. Our findings reveal that neural circuitry, via mosaic innervation of the V-SVZ, can recruit distinct NSC pools, allowing on-demand neurogenesis in response to physiology and environmental signals.

Neural stem cells dynamically sense and integrate diverse signals in the microenvironment to modulate adult neurogenesis. The adult ventricular-subventricular zone (V-SVZ) stem cell niche adjacent to the lateral ventricles in the brain generates thousands of olfactory bulb (OB) interneurons each day (fig. S1A) (*1*, *2*). The extensive heterogeneity of adult neural stem cells is just emerging (*3*). Neural stem cells (NSCs) residing in different regions of the V-SVZ have an intrinsic regional identity that determines the subtype of OB interneuron they produce (*3*). However, whether V-SVZ niche components and signals are regionalized and differentially regulate distinct pools of adult NSCs is largely unknown.

Adult V-SVZ NSCs are radial cells that express glial fibrillary acidic protein (GFAP) (*4*, *5*). V-SVZ NSCs are mostly quiescent but upon activation divide to generate transit-amplifying cells and in turn neuroblasts that migrate to the OB (*4*, *6*). Extrinsic cues are thought to regulate the transition from the quiescent- to activated-NSC state, but the specific signals that trigger activation of quiescent NSCs (qNSCs) are poorly understood. To identify activators of qNSCs, we tested the Tocriscreen Mini Library (Tocris) for up-regulation of Nestin and MCM2 in prospectively purified qNSCs (*6*) and chose ICI 204448 (ICI), an agonist of the κ-opioid receptor (Oprk1), for further analysis. ICI significantly increased Nestin$^+$MCM2$^+$ qNSC-derived clones, as did the endogenous opioid ligand β-endorphin (Fig. 1, A to C, and fig. S1, B and C). This effect was blocked by the Oprk1-specific antagonist DIPPA (Fig. 1C and fig. S1D). In vivo, acute intraventricular administration of ICI or DIPPA (fig. S1E) selectively affected proliferation in the anterior ventral (AV) V-SVZ, a domain containing Nkx2.1$^+$ NSCs (*7*, *8*). ICI increased, and DIPPA decreased, proliferation of AV V-SVZ NSCs (GFAP$^+$Ki67$^+$) (fig. S1, M to P) but had no effect on transit-amplifying cells (GFAP$^-$Ki67$^+$DCX$^-$) and neuroblasts (DCX$^+$) (fig. S1Q) or anterior dorsal (AD) V-SVZ NSCs (fig. S1, I to L). Moreover, only proliferation of Nkx2.1$^+$ NSCs was affected (Fig. 1D and fig. S1, F to H), with no change in total number of GFAP$^+$Nkx2.1$^+$ NSCs (Fig. 1E). Oprk1 immunostaining was also enriched in the AV V-SVZ as compared with AD V-SVZ (fig. S1, R and S) and predominantly expressed in NSCs (fig. S1T).

To identify an in vivo source of β-endorphin, we immunostained coronal brain sections from adult *GFAP::GFP* mice (GFP, green fluorescent protein) (*9*). β-endorphin expression was regionalized, labeling the AV—but not AD—V-SVZ and encompassed the entire Nkx2.1$^+$ domain (Fig. 1, F and G, and fig. S2, A to E). Moreover, β-endorphin fibers occasionally directly contacted AV NSCs and colocalized with the presynaptic marker VAMP2 (fig. S3). No β-endorphin$^+$ somas were detected in the vicinity of the AV V-SVZ, suggesting a long-range, neuronal source (Fig. 1G and fig. S2B). Because β-endorphin is a posttranslational cleavage product of proopiomelanocortin (POMC) (*10*), we investigated whether POMC-expressing neurons in the arcuate nucleus of the hypothalamus innervate the V-SVZ using viral approaches. An adeno-associated virus (AAV) expressing yellow fluorescent protein (YFP) (AAV-Flex-YFP) (*11*, *12*) in a cre-dependent manner was injected into the hypothalamus of *Pomc-cre* mice (Fig. 2, A and C) (*13*) to selectively transduce POMC$^+$ neurons (fig. S4A). Hypothalamic POMC$^+$ neurons (YFP$^+$) sent long-distance projections to the V-SVZ, innervating the AV but not other V-SVZ regions (Fig. 2, B and D, and fig. S4, B and C).

To determine whether hypothalamic POMC$^+$ neurons regulate adult NSC proliferation in vivo, we used viral approaches to selectively ablate POMC$^+$ neurons or acutely manipulate their activity. To ablate POMC neurons, an AAV that expresses cleaved caspase-3 in a cre-dependent manner (AAV-Flex-Casp3) (*14*), or control AAV-Flex-YFP, was unilaterally injected into the hypothalamus of *Pomc-cre* mice (Fig. 2A and fig. S5A). Seven weeks after AAV-Flex-Casp3 injection, the number of POMC$^+$ hypothalamic neurons was

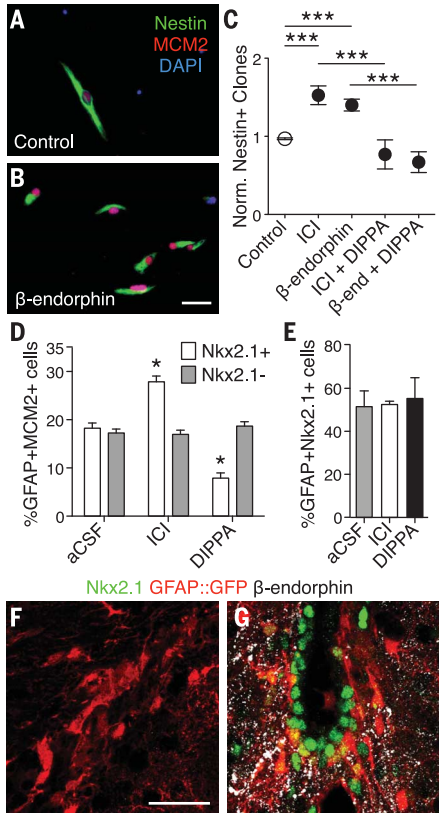

Fig. 1. Regionalized response of AV V-SVZ Nkx2.1$^+$ NSCs to opioid ligands. (**A** and **B**) Representative images of activated qNSCs in vitro [Nestin$^+$, MCM2$^+$, and DAPI$^+$ (4′,6-diamidino-2-phenylindole)] in (A) control or (B) β-endorphin–treated conditions. (**C**) Proportion of Nestin$^+$ qNSC clones, normalized to control, upon agonist and/or antagonist treatment. ICI 204448 (ICI), selective Oprk1 agonist; DIPPA, Oprk1-specific antagonist. (**D**) Quantification of Nkx2.1$^+$ and Nkx2.1$^-$ proliferating NSCs (Nkx2.1$^+$GFAP$^+$MCM2$^+$/Nkx2.1$^+$GFAP$^+$ and Nkx2.1$^-$GFAP$^+$MCM2$^+$/Nkx2.1$^-$GFAP$^+$ cells) in the AV V-SVZ upon acute administration of artificial cerebrospinal fluid (aCSF), ICI, and DIPPA. (**E**) Proportion of GFAP$^+$Nkx2.1$^+$/GFAP$^+$ cells in the AV V-SVZ. (**F** and **G**) Confocal projections of (F) dorsal and (G) ventral V-SVZ immunostained for GFAP::GFP, Nkx2.1, and β-endorphin. Scale bars, 30 μm (B) and 40 μm (F).

[1]Department of Genetics and Development, Columbia University, New York, NY 10032, USA. [2]Department of Pathology and Cell Biology, Columbia University, New York, NY 10032, USA. [3]Biozentrum, University of Basel, CH 4056 Basel, Switzerland.
*Corresponding author. Email: fiona.doetsch@unibas.ch

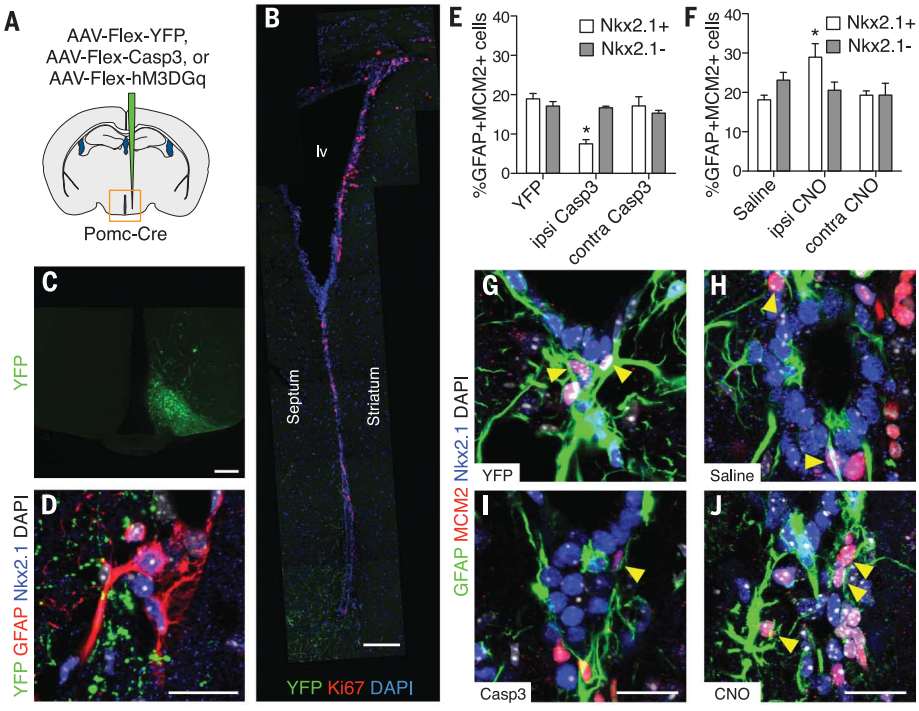

Fig. 2. Hypothalamic POMC$^+$ neurons innervate the AV V-SVZ and promote the proliferation of Nkx2.1$^+$ NSCs. (**A**) AAV-Flex-YFP, AAV-Flex-Casp3, or AAV-Flex-hM3DGq-mCherry were injected unilaterally into the hypothalamus of *Pomc-cre* mice. (**B**) Confocal projection of V-SVZ from AAV-Flex-YFP–injected *Pomc-cre* mouse immunostained for YFP, Ki67, and DAPI. YFP$^+$ fibers are present in the septum and target ventral V-SVZ, but not other V-SVZ regions. lv, lateral ventricle. (**C**) Confocal image showing unilateral YFP expression in the hypothalamic arcuate nucleus. (**D**) Confocal projection showing YFP$^+$ fibers in the AV V-SVZ in the Nkx2.1 NSC domain. (**E** and **F**) Quantification of Nkx2.1$^+$ and Nkx2.1$^-$ proliferating NSCs (Nkx2.1$^+$GFAP$^+$MCM2$^+$/Nkx2.1$^+$GFAP$^+$ and Nkx2.1$^-$GFAP$^+$MCM2$^+$/Nkx2.1$^-$GFAP$^+$ cells) in AV V-SVZ after ablating (E) or activating POMC neurons with DREADDs (F). (**G** to **J**) Confocal images of NSCs in AV V-SVZ after POMC neuron ablation [(G) and (I)] or activation [(H) and (J)]. Arrowheads indicate dividing Nkx2.1$^+$GFAP$^+$MCM2$^+$ NSCs. Scale bars, 200 μm (C), 100 μm (B), and 20 μm [(D), (I), and (J)].

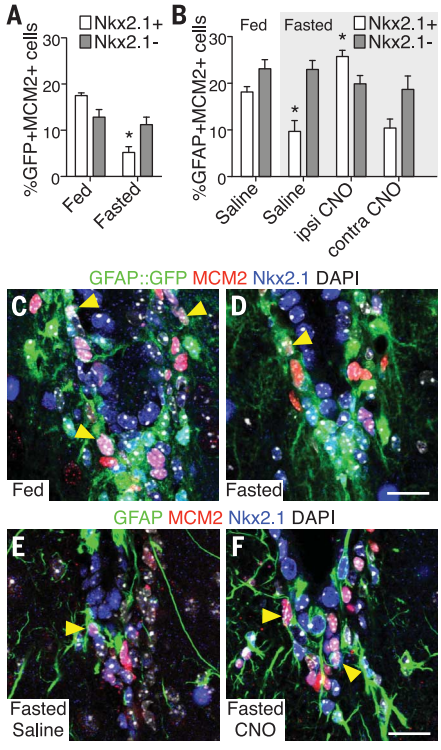

Fig. 3. Hunger and satiety regulate Nkx2.1$^+$ NSC proliferation in AV V-SVZ via POMC neuron activity. (**A**) Proportion of Nkx2.1$^+$ and Nkx2.1$^-$ proliferating NSCs (Nkx2.1$^+$GFAP::GFP$^+$MCM2$^+$/Nkx2.1$^+$GFAP::GFP$^+$ and Nkx2.1$^-$GFAP::GFP$^+$MCM2$^+$/Nkx2.1$^-$GFAP::GFP$^+$ cells) in the AV V-SVZ of fed and fasted *GFAP::GFP* animals. (**B**) Proportion of Nkx2.1$^+$ and Nkx2.1$^-$ proliferating NSCs (Nkx2.1$^+$GFAP$^+$MCM2$^+$/Nkx2.1$^+$GFAP$^+$ and Nkx2.1$^-$GFAP$^+$MCM2$^+$/Nkx2.1$^-$GFAP$^+$ cells) in the AV V-SVZ of fed and fasted *Pomc-cre* animals injected with AAV-Flex-hM3DGq-mCherry and treated with saline or CNO. (**C** and **D**) Confocal images of the AV V-SVZ of (C) fed and (D) fasted *GFAP::GFP* animals. Arrowheads indicate dividing Nkx2.1$^+$GFAP::GFP$^+$MCM2$^+$ NSCs. (**E** and **F**) Confocal images of the AV V-SVZ of fasted AAV-Flex-hM3DGq-mCherry–injected *Pomc-cre* animals treated with (E) saline or (F) CNO. Arrowheads indicate dividing Nkx2.1$^+$GFAP$^+$MCM2$^+$ NSCs. Scale bars, 20 μm.

reduced by 66% (fig. S5, B and C). This led to a decrease in NSC proliferation by 61% specifically in the AV V-SVZ of AAV-Flex-Casp3–injected animals (fig. S5, E to H), with only Nkx2.1$^+$ NSCs affected (Fig. 2, E, G, and I), and a concomitant decrease in transit-amplifying cells (fig. S5H). The total number of GFAP$^+$Nkx2.1$^+$ V-SVZ cells was unchanged between AAV-Flex-Casp3 and control animals (fig. S5D), indicating that the decrease in proliferating Nkx2.1$^+$ NSCs is not due to cell death. The effects were restricted to the AV V-SVZ ipsilateral to the ablation, suggesting that they are not due to systemic changes (Fig. 2E and fig. S5H).

We next acutely increased the activity of POMC neurons using activating DREADDs (designer receptors exclusively activated by designer drugs) (*15*). AAV-Flex-hM3DGq-mCherry (*16*) was unilaterally injected into the hypothalamus of *Pomc-cre* mice. Three weeks later, upon administration of clozapine N-oxide (CNO), the number of active (c-fos$^+$mCherry$^+$) hypothalamic POMC neurons doubled (fig. S5, I to M). In the V-SVZ, Nkx2.1$^+$ NSC proliferation was specifically increased on the ipsilateral side (Fig. 2, F, H, and J), with no change in total GFAP$^+$Nkx2.1$^+$ NSCs (fig. S5N). Virally transduced POMC neurons directly contacted NSCs as well as niche cells (fig. S4, D to L). As such, the effect on NSC proliferation caused by modulating hypothalamic POMC neuron activity could be due to direct stimulation of NSCs, volume transmission, or via niche cells.

Hypothalamic POMC$^+$ neurons are a key component of a feedback circuit that regulates feeding behavior during hunger and satiety (*17*, *18*), suggesting that these physiological states may affect regional NSC proliferation. POMC$^+$ neuron activity is increased upon feeding and decreased during fasting periods (fig. S6, A and B). To test whether hunger and satiety states regulate NSC proliferation in the AV V-SVZ, we quantified NSC proliferation in *GFAP::GFP* mice that were either ad libitum fed, fasted, or fasted then refed (fig. S6C). Hypothalamic POMC$^+$ neuron activity (β-endorphin$^+$ c-fos$^+$ cells) decreased by 56% in fasted animals and returned to baseline upon refeeding (fig. S6, D to G). In the AV V-SVZ, NSC proliferation (GFAP::GFP$^+$ MCM2$^+$) decreased by 68% in fasted animals and recovered to control levels upon refeeding (fig. S6, L to O). NSC proliferation in the AD V-SVZ (fig. S6, H to K), total numbers of GFAP::GFP$^+$ cells, transit-amplifying cells, or neuroblasts in the AV V-SVZ were not affected (fig. S6P). The decrease in NSC proliferation in fasted animals was specific to Nkx2.1$^+$ NSCs (Fig. 3, A, C, and D), whereas the total proportion of Nkx2.1$^+$ NSCs in the AV V-SVZ was unchanged (fig. S6Q). This decrease was fully rescued by activating POMC neurons during fasting with DREADDs (Fig. 3, B, E, and F, and fig. S7) only on the ipsilateral side. Therefore, hunger and satiety states specifically regulate Nkx2.1$^+$ NSC proliferation

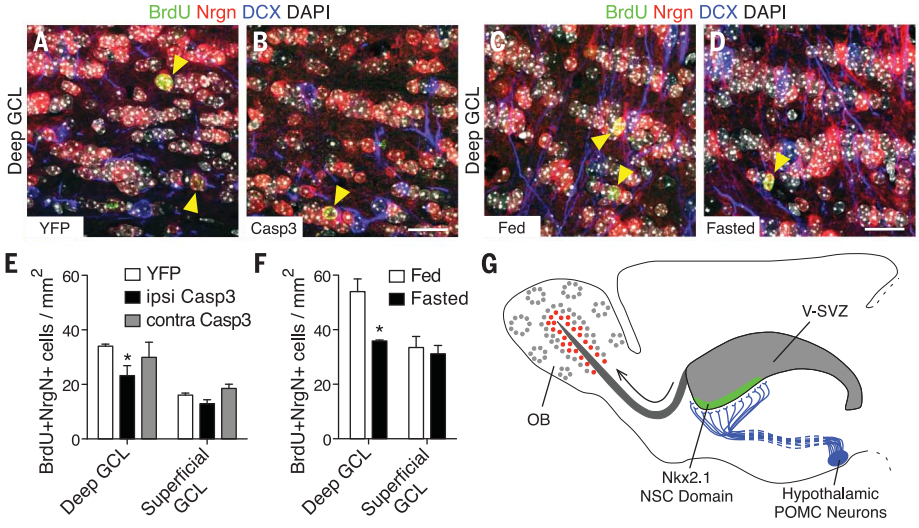

Fig. 4. Hypothalamic POMC$^+$ neurons regulate the production of deep GCL interneurons in the OB. (**A** to **D**) Confocal images of deep GCL in OB of (A) AAV-Flex-YFP–injected and (B) AAV-Flex-Casp3–injected *Pomc-cre* animals, and (C) fed and (D) fasted animals. Arrowheads indicate BrdU$^+$Nrgn$^+$DCX$^-$ cells. (**E** and **F**) Quantification of BrdU$^+$Nrgn$^+$DCX$^-$ interneurons in the deep and superficial GCL, in (E) AAV-injected animals and (F) fed and fasted animals. (**G**) Model showing hypothalamic POMC$^+$ neurons (blue) selectively innervate the Nkx2.1 NSC domain (green) in the anterior ventral V-SVZ and modulate the proliferation of Nkx2.1$^+$ NSCs during hunger and satiety states, in an activity-dependent manner, regulating the production of deep GCL interneurons (red dots) in the OB. The exact trajectory of POMC$^+$ neuron projections to the V-SVZ is not known and is therefore shown as dashed lines. Scale bars, 10 μm.

in the AV V-SVZ via modulating POMC neuron activity.

NSCs residing in different regions of the V-SVZ give rise to distinct OB interneuron subtypes (*3*). Adult-born OB interneurons can be classified by their position within the granule cell layer (GCL) or glomerular layer (GL) and expression of specific molecular markers (*3*). Adult Nkx2.1$^+$ NSCs in the AV V-SVZ generate deep GCL interneurons (*7*, *8*, *19*) that express Neurogranin (Nrgn) (*20*). To test whether hypothalamic POMC$^+$ neurons regulate the production of Nrgn$^+$ deep GCL interneurons, we examined the generation of new neurons either after ablation of POMC$^+$ neurons, or during fasting. Mice were pulsed with BrdU 3 weeks after ablation of POMC neurons (fig. S8A) or during fasting (fig. S9A), and the proportions of BrdU$^+$ OB interneuron subtypes were quantified 30 days later. In both ablation and fasting paradigms, BrdU$^+$Nrgn$^+$DCX$^-$ deep GCL interneurons decreased 32 and 33%, respectively (Fig. 4, A to F, and figs. S8, L and M, and S9, L and M), but adult-generated Nrgn$^+$ and CalR$^+$ superficial GCL—and CalR$^+$, TH$^+$, or CalB$^+$ periglomerular interneurons—did not change (figs. S8, B to K, and S9, B to K). In the POMC ablation paradigm, these effects were specific to the ipsilateral side (Fig. 4E). Taken together, our results reveal that hypothalamic POMC$^+$ neurons provide long-range regionalized innervation to the AV V-SVZ and regulate the proliferation of Nkx2.1$^+$ NSCs and the production of deep GCL interneurons (Fig. 4G) via their activity. Hunger and satiety impinge on the activity of this circuit. As such, availability of food in the wild may affect the quiescence or recruitment of specific stem cell pools to alter the rate of neurogenesis, leading to specific adaptations in OB circuitry.

Our study demonstrates that heterogeneity in the V-SVZ encompasses both the intrinsic spatial identity of NSCs (*3*) and regionalization of stem cell niche components. Although several types of neurons innervate the V-SVZ niche (*21*–*25*), their effect on regional NSC subtypes is unknown. Our findings reveal that neuronal innervation can target different spatial domains in the V-SVZ stem cell niche and selectively affect distinct pools of adult NSCs. Neural circuits from diverse brain regions may therefore underlie the regulation of heterogeneous adult NSCs by mosaically innervating the V-SVZ stem cell niche. Moreover, our findings suggest that hypothalamic neural circuits link physiological states to regional NSC proliferation and the production of discrete OB interneuron subtypes. As such, they provide a logic of how diverse physiological states may lead to on-demand adult neurogenesis.

REFERENCES AND NOTES

1. L. C. Fuentealba, K. Obernier, A. Alvarez-Buylla, *Cell Stem Cell* **10**, 698–708 (2012).
2. V. Silva-Vargas, E. E. Crouch, F. Doetsch, *Curr. Opin. Neurobiol.* **23**, 935–942 (2013).
3. Z. Chaker, P. Codega, F. Doetsch, *Wiley Interdiscip. Rev. Dev. Biol.* **5**, 640–658 (2016).
4. F. Doetsch, I. Caillé, D. A. Lim, J. M. García-Verdugo, A. Alvarez-Buylla, *Cell* **97**, 703–716 (1999).
5. Z. Mirzadeh, F. T. Merkle, M. Soriano-Navarro, J. M. Garcia-Verdugo, A. Alvarez-Buylla, *Cell Stem Cell* **3**, 265–278 (2008).
6. P. Codega *et al.*, *Neuron* **82**, 545–559 (2014).
7. F. T. Merkle *et al.*, *Nat. Neurosci.* **17**, 207–214 (2014).
8. R. N. Delgado, D. A. Lim, *Dev. Biol.* **407**, 265–274 (2015).
9. L. Zhuo *et al.*, *Dev. Biol.* **187**, 36–42 (1997).
10. R. G. Allen *et al.*, *J. Neurosci.* **21**, 5864–5870 (2001).
11. D. Atasoy, Y. Aponte, H. H. Su, S. M. Sternson, *J. Neurosci.* **28**, 7025–7030 (2008).
12. P. S. Kunwar *et al.*, *eLife* **4**, e06633 (2015).
13. T. J. McHugh *et al.*, *Science* **317**, 94–99 (2007).
14. C. F. Yang *et al.*, *Cell* **153**, 896–909 (2013).
15. G. M. Alexander *et al.*, *Neuron* **63**, 27–39 (2009).
16. M. J. Krashes *et al.*, *J. Clin. Invest.* **121**, 1424–1428 (2011).
17. L. M. Zeltser, R. J. Seeley, M. H. Tschöp, *Nat. Neurosci.* **15**, 1336–1342 (2012).
18. Y. Aponte, D. Atasoy, S. M. Sternson, *Nat. Neurosci.* **14**, 351–355 (2011).
19. F. T. Merkle, Z. Mirzadeh, A. Alvarez-Buylla, *Science* **317**, 381–384 (2007).
20. S. Gribaudo, S. Bovetti, D. Garzotto, A. Fasolo, S. De Marchis, *J. Comp. Neurol.* **517**, 683–694 (2009).
21. G. U. Höglinger *et al.*, *Nat. Neurosci.* **7**, 726–735 (2004).
22. J. B. Lennington *et al.*, *J. Neurosci.* **31**, 13078–13087 (2011).
23. P. Paez-Gonzalez, B. Asrican, E. Rodriguez, C. T. Kuo, *Nat. Neurosci.* **17**, 934–942 (2014).
24. C. K. Tong *et al.*, *Cell Stem Cell* **14**, 500–511 (2014).
25. S. Z. Young, C. A. Lafourcade, J.-C. Platel, T. V. Lin, A. Bordey, *Front. Cell. Neurosci.* **8**, 10 (2014).

ACKNOWLEDGMENTS

The authors thank the Columbia Herbert Irving Comprehensive Cancer Center Flow Cytometry Core for assistance with fluorescence-activated cell sorting; the JP Sulzberger Columbia Genome Center for assistance with small-molecule screening; R. Hen and M. Kheirbek for viruses, *Pomc-cre* mice, and discussion; P. Scheiffele for VAMP2 antibodies and discussion; members of the Doetsch and Wichterle laboratories for discussion; and V. Silva-Vargas and A. Delgado for comments on the manuscript. This work was supported by NIH National Institute of Neurological Disorders and Stroke (NINDS) grant NS053884 (F.D.), NIH NINDS grant NS074039 (F.D.), New York State Stem Cell Science contract C024287 (F.D.), the Leona M. and Harry B. Helmsley Charitable Trust (F.D.), and NIH NINDS fellowship F31NS089252 (A.P.). Work was also supported by the Jerry and Emily Spiegel Laboratory for Cell Replacement Therapies and the University of Basel. The supplementary materials contain additional data. A.P. and F.D. designed experiments; A.P. and Z.C. performed and analyzed experiments; and A.P., Z.C., and F.D. wrote the manuscript.

SUPPLEMENTARY MATERIALS

www.sciencemag.org/content/356/6345/1383/suppl/DC1
Materials and Methods
Figs. S1 to S9
Reference (*26*)

10 November 2016; accepted 1 June 2017
Published online 15 June 2017
10.1126/science.aal3839

Hypothalamic regulation of regionally distinct adult neural stem cells and neurogenesis

Alex Paul, Zayna Chaker and Fiona Doetsch

Science **356** (6345), 1383-1386.
DOI: 10.1126/science.aal3839originally published online June 15, 2017

Specialization in brain neurogenic niche

The adult mammalian brain generates neurons from the subventricular zone (SVZ). In mice, Paul *et al.* were able to link environmental signals with the type of neurons that are generated and showed that anatomical subspecialization occurrs in the SVZ. Neural circuits that respond to hunger or satiety enervate a subregion of the SVZ and retune the production of new olfactory neurons just from that portion of the subventricular niche.

Science, this issue p. 1383